Journal of Food Engineering 100 (2010) 535–544

Contents lists available at ScienceDirect

Journal of Food Engineering

journal homepage: www.elsevier.com/locate/jfoodeng

Porous multiphase approach for baking process – Explicit formulation of evaporation rate

A. Ousegui [a,*], C. Moresoli [b], M. Dostie [c], B. Marcos [a]

[a] Département de génie chimique et de génie biotechnologique, Faculté de génie, Université de Sherbrooke, Québec, Canada J1K 2R
[b] Department of Chemical Engineering, University of Waterloo, Waterloo, Ontario, Canada N2L 3G1
[c] Laboratoire des technologies de l'énergie, LTE-Hydro-Québec, Shawinigan, Québec, Canada G9N 7N5

ARTICLE INFO

Article history:
Received 2 March 2010
Received in revised form 10 May 2010
Accepted 12 May 2010
Available online 16 May 2010

Keywords:
Baking process
Heat transfer
Mass transfer
Porous media
Phase change
Evaporation rate
Non equilibrium approach

ABSTRACT

A multiphase model for simultaneous heat and mass transfer in porous medium was developed to simulate the baking process of a bread product. The model was based on Fourier's law for conductive heat transfer and Darcy's and Fick's laws for mass transfer of liquid (water) and gas (water vapour and CO_2) phases. Explicit formulation was adopted for the evaporation rate allowing direct solution of the system of equations. The use of the non equilibrium approach, allowed the implementation of the model in commercial software. Numerical Finite Element Method (FEM) scheme was used to solve the equations. The model was compared with experimental results reported in literature. Results show a good agreement between experimental and numerical results. Sensitivity analysis of the effect of the evaporation rate constant and process operating conditions on the temperature and moisture content were conducted and showed that the baking process was affected mainly by the convective heat transfer and the product initial moisture characteristics.

1. Introduction

Baking process is an important procedure in bread production. The final product quality attributes (texture, color) are determined during the baking operation (oven temperature, moisture content, and emissivity). In addition, baking is considered as a major energy consuming process compared to other conventional food processes (Fellows, 1996). Therefore, significant experimental and modeling efforts have been conducted for understanding and subsequently generating solutions for baking processes by calculating optimal operation strategies that serve as a basis for process and unit operation design (Hadiyanto et al., 2008).

From a modeling perspective, baking is treated as a coupled heat and mass transfer process (one phase or two phases, i.e. liquid and vapour) between the baking product and ambient air. Conventional models (Zhou, 2005) based only on diffusive transfer are unable to predict the rapid heat transfer during baking and the increase of liquid water content in the center of the dough during the early stages of the process; a phenomenon already observed experimentally (Thorvaldsson and Skjöldebrand, 1998).

Several papers (Zhou, 2005; Datta, 2007a; Mondal and Datta, 2008) with some differences in evaporation rate expressions as we will see later – show that the "evaporation–condensation" approach developed by Thorvaldsson and Janestad (1999) is more successful for modeling heat and moisture transfer during baking. The approach is a multiphase flow model consisting of three coupled balance equations for the simultaneous heat transfer, liquid water diffusion and water vapour diffusion, respectively. However, further investigations using the initial form of the model report serious numerical difficulties related to the type of numerical schemes, time step size, and meshes methods used (uniform, non-uniform) in converging to a solution (Zhou, 2005), and also an inadequacy in satisfying the mass conservation (Zhang and Datta, 2004). Thus, an improved model was suggested by replacing the instantaneous phase change of liquid to vapour and by introducing an evaporation rate term (Huang et al., 2007). Other improvements were also made (Zhang et al., 2005, 2007; Zhang and Datta, 2006; Hadiyanto et al., 2007, 2008) which could be categorized as equilibrium approach and include:

(1) The incorporation of the porous texture of the dough and the convective transport through the dough,
(2) The inclusion of other gases in the gas phase (specifically CO_2).
(3) The incorporation of the dough volumetric change during baking.

Nevertheless, this equilibrium approach needs a special treatment of the system of mathematical equations since the

* Corresponding author. Tel.: +1 819 821 80 00x62 672.
E-mail address: Abdellah.ousegui@usherbrooke.ca (A. Ousegui).

0260-8774/$ - see front matter © 2010 Published by Elsevier Ltd.
doi:10.1016/j.jfoodeng.2010.05.003

Nomenclature

a_w	water activity (–)
C	molar density of gas mixture (mol/m^3)
c_p	specific heat capacity (J/kg K)
D	mass diffusivity (m^2/s)
h_m	convective mass transfer coefficient (m/s)
h_t	overall heat transfer coefficient (W/m^2 K)
h_v	convective heat transfer coefficient (W/m^2 K)
$\dot{I}$	evaporation rate (kg/m^3 s)
K	non-equilibrium evaporation constant (s^{-1})
k	thermal conductivity (W/m K)
M	total moisture content dry basis (–)
M_c	molecular weight of CO_2 gas (kg/mol)
M_v	molecular weight of water vapour (kg/mol)
n	normal direction when without subscripts
n	total flux when with subscripts (kg/m^2 s)
P	total pressure (Pa)
p	partial pressure (Pa)
p_s	saturation pressure (Pa)
R	universal constant ideal gas 8.314 (J/mol K)
S	saturation (–)
T	temperature (K)
t	time (s)
u_g	gas phase velocity (m/s)
V	volume (m^3)
x	coordinate (m)
y	coordinate (m)

Greek letters

ϕ	porosity (–)
ρ	density (kg/m^3)
κ	permeability (m^2)
μ	dynamic viscosity (Pa/s)
λ	latent heat of evaporation (J/kg)
ε	emissivity
σ	Stefan–Boltzmann constant (W/m^2 K^4)

Subscripts

0	initial state
c	CO_2 gas
eq	equilibrium
db	dry basis
eff	effective
g	gas phase
i	intrinsic
inf	ambient
r	relative
s	solid
s	surface
tot	total
v	vapour water
w	liquid water
wt	wet basis

evaporation rate is included as an unknown parameter (Zhang and Datta, 2004), which remains as a major challenge when commercial softwares are used to model the process.

To overcome this problem, recently an approach using explicit formulation of the evaporation rate "non-equilibrium approach" (Halder et al., 2007b) for the frying operation was proposed, based on the expression developed by Fang and Ward (1999), and gave good predictions of the heat and moisture transfer during the process. Conceptually, the evaporation rate is related, not necessarily linearly, to the difference between the equilibrium vapour density (or pressure) and the actual local vapour density (or pressure) at that instant.

The main objectives of this paper are:

- Develop a multiphase model based on the "evaporation–condensation" approach that takes into account the porosity of the product and the mass transfer by capillarity (porous capillary) to simulate the baking process, that is easy to implement with a commercial software package.
- Validate the model estimates with experimental measurements of temperature and moisture of baking products reported in literature.
- Investigate the impact of oven operating conditions on the baking process.

2. Model development

2.1. Assumptions

During all the steps of the baking process, the product consists of three phases: solid (dry matter), liquid water, and gas (water vapour and CO_2 gas). All phases are assumed to have the same temperature at any spatial location. Water vapour and CO_2 are assumed to be ideal gases. Water vapour and CO_2 are driven by convective flow due to the total gas pressure gradient and "diffusion" due to the concentration gradient.

Liquid water is strongly bound to starch, so there is no pressure driven liquid water flow in baking and the only transfer mechanism for liquid water is "capillary diffusion". CO_2 generation is not considered and consequently volume expansion during baking due to CO_2 generation is not considered. Evaporation–condensation rate is linearly related to the difference between equilibrium vapour density and local vapour density.

2.2. Governing equations for mass and energy conservation

The governing equations will be written in terms of apparent porosity, water and gas saturation. The apparent porosity and saturation are defined from the volume of each phase V_w, V_g and V_s. The total volume is the sum of the volume of the three phases:

$$V_{tot} = V_w + V_g + V_s \tag{1}$$

The apparent porosity represents the ratio between the combined volume fraction of water and gases and the total volume:

$$\phi = \frac{V_w + V_g}{V_{tot}} \tag{2}$$

Water and gas saturation represent the fraction of the pore volume occupied by each phase (water and gas):

$$S_w = \frac{V_w}{V_w + V_g} = \frac{V_w}{\phi V_{tot}} \tag{3}$$

$$S_g = \frac{V_g}{V_w + V_g} = \frac{V_g}{\phi V_{tot}} = 1 - S_w \tag{4}$$

The mass concentrations of liquid water, water vapour and CO_2 gas are related to the saturation, respectively, by:

$$\frac{m_w}{V_{tot}} = \frac{\rho_w V_w}{V_{tot}} = \rho_w S_w \phi \quad (5)$$

$$\frac{m_v}{V_{tot}} = \frac{\rho_v V_v}{V_{tot}} = \rho_v S_g \phi \quad (6)$$

$$\frac{m_c}{V_{tot}} = \frac{\rho_c V_c}{V_{tot}} = \rho_c S_g \phi \quad (7)$$

For the gas mixture, the total pressure is equal to the sum of the partial pressures of CO_2 and vapour and the mass concentration of the gas mixture is obtained from the ideal gas law:

$$P = p_v + p_c \quad (8)$$

$$\rho_g = \frac{m_v + m_c}{V_g} = \rho_v + \rho_c = \frac{p_v M_v}{RT} + \frac{p_c M_c}{RT} \quad (9)$$

The moisture content (dry basis) M is related to the water saturation S_w, by:

$$M = \frac{\rho_w S_w \phi}{\rho_s (1-\phi)} \quad (10)$$

where ρ_s is the density of the solid phase in the product.

The mass conservation for each of the three phases making up the porous medium is given by:

$$\frac{\partial(\rho_w S_w \phi)}{\partial t} + \vec{\nabla} \cdot (\vec{n}_w) = -\dot{I} \quad (11)$$

$$\frac{\partial(\rho_v S_g \phi)}{\partial t} + \vec{\nabla} \cdot (\vec{n}_v) = \dot{I} \quad (12)$$

$$\frac{\partial(\rho_c S_g \phi)}{\partial t} + \vec{\nabla} \cdot (\vec{n}_c) = 0 \quad (13)$$

n_w represents the liquid water flux, as mentioned in Section 1.1, no flow of liquid water by convection is occurring, so:

$$\vec{n}_w = -D_w \rho_w \phi \vec{\nabla} S_w \quad (14)$$

$\dot{I}$ is the rate of evaporation (kg m^{-3} s^{-1}) which represents the mass of liquid water that becomes vapour per unit volume and time. The rate of evaporation $\dot{I}$ can be either positive during the evaporation process or negative during the condensation process.

n_v and n_c, the total flux of water vapour and CO_2, respectively, are described by Darcy flow flux (Bear, 1972) and diffusion flux (Bird et al., 2001):

$$\vec{n}_v = -\rho_v \frac{\kappa_g}{\mu_g} \vec{\nabla} P - D_{eff} \frac{C^2}{\rho_g} M_c M_v \vec{\nabla}\left(\frac{p_v}{P}\right) \quad (15)$$

$$\vec{n}_c = -\rho_c \frac{\kappa_g}{\mu_g} \vec{\nabla} P - D_{eff} \frac{C^2}{\rho_g} M_c M_v \vec{\nabla}\left(\frac{p_c}{P}\right) \quad (16)$$

From the first term of Eqs. (15) and (16), the velocity of the gas phase is defined by Darcy's law:

$$\vec{u}_g = -\frac{\kappa_g}{\mu_g} \vec{\nabla} P \quad (17)$$

The energy conservation gives the following equation:

$$\rho_{eff} c_{p_{eff}} \frac{\partial T}{\partial t} + \vec{\nabla} \cdot (\rho_g c_{pg} T \cdot \vec{u}_g) = \vec{\nabla} \cdot (k_{eff} T) - \lambda \dot{I} \quad (18)$$

λ is the latent heat of evaporation, the expression of the other thermophysical properties will be detailed in Section 3.2.

The system of Eqs. (11), (12), (13), and (18) has four equations and five unknowns ($\rho_w \phi S_w, \rho_v \phi S_g, \rho_c \phi S_g$, T and $\dot{I}$); an additional equation that gives a relation between the evaporation rate $\dot{I}$ and the others variables, is required to close the system as will be discussed in Section 1.4.

2.3. Study cases and experimental conditions

The model is validated for two experimental cases: case 1 is a short cylindrical bread (Zhang et al., 2005) and case 2 is a French baguette (Purlis and Salvadori, 2009). In both cases, the initial conditions for the mass and energy conservation equations are deduced from the initial humidity (M_0), the initial density of dough ρ_0, the initial gas volume ratio V_g/V_t and the initial product temperature T_0. The initial condition for the energy equation is simply:

$$T = T_0 \quad (19)$$

Expressions of the initial conditions for liquid water, water vapour and CO_2 gas are given in Eqs. (20)–(22) and detailed information is given in Appendix A for the calculation of these quantities from experimentally available data.

$$\text{For Eq.(11)} \quad (\rho_w \phi S)_{t=0} = \rho_w \phi S_{w0} \quad (20)$$

$$\text{For Eq.(12)} \quad (\rho_v S_g \phi)_{t=0} = \frac{p_{v0} M_v}{RT_0} \phi (1 - S_{w0}) \quad (21)$$

$$\text{For Eq.(13)} \quad (\rho_c S_g \phi)_{t=0} = \frac{(P_{atm} - p_{v0}) M_c}{RT_0} \phi (1 - S_{w0}) \quad (22)$$

p_{v0} is deduced from Eq. (30), for $T = T_0$ and $M = M_0$.

2.3.1. Product dimension and boundary conditions: case 1 short cylindrical bread (Zhang et al., 2005)

The bread dough sample is a short cylinder positioned vertically with a 7 cm diameter and 3.5 cm height. The bread was baked a domestic oven at a temperature of 190 °C, for a period of 15 min. For symmetry and axi symmetry reasons, a quarter of the product was simulated (see Fig. 1)

On the surfaces $\partial\Omega_{3,4}$,

$$-\vec{n}_w \cdot \vec{n} = h_m \phi S_w (\rho_{v,s} - \rho_{v,\inf}) \quad (23)$$

$$-\vec{n}_v \cdot \vec{n} = h_m \phi S_g (\rho_{v,s} - \rho_{v,\inf}) \quad (24)$$

$$\rho_c S_g \phi = (P_{atm} - p_v) \frac{M_c}{RT} \quad (25)$$

$$-k_{eff} \vec{\nabla} T \cdot \vec{n} = h_t (T_{\inf} - T_s) \quad (26)$$

where h_t is the overall heat transfer coefficient including convective and radiative heat transfer mode.

For the surfaces $\partial\Omega_1$ and $\partial\Omega_2$ a symmetry boundary condition was used:

$$\vec{\Gamma} \cdot \vec{n} = 0 \quad (27)$$

where $\vec{\Gamma}$ represents the vector of the quantities presented above.

Point with coordinate (0, 0) represents the center of the whole product.

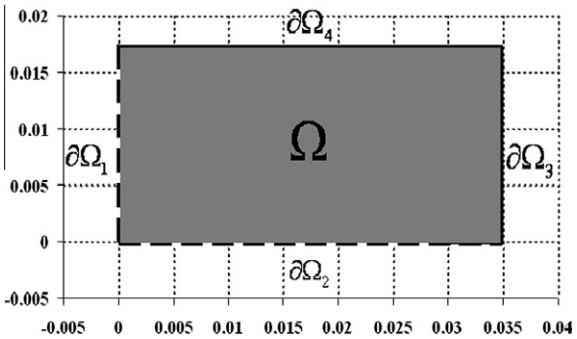

Fig. 1. Geometry of the bread baking product investigated by Zhang et al. (2005).

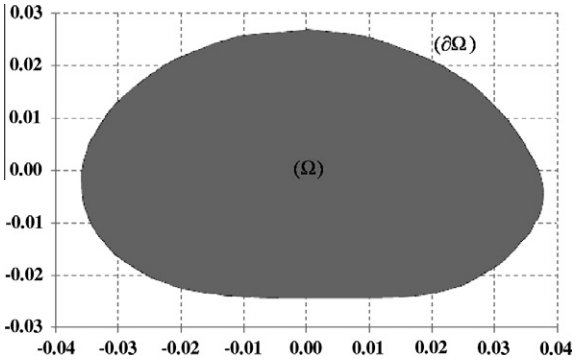

Fig. 2. Geometry of the bread baking product investigated by Purlis and Salvadori (2009).

Table 1
Initial and boundary conditions of study cases.

	Initial conditions		Boundary conditions			
	T_0	M_0	T_{inf}	h	h_m	Convection mode
Case 1	27	0.54	190	10	0.01	N/A
	25	0.64	180	12	0.0136	Forced
Case 2	25	0.64	200	12	0.0236	Forced
	25	0.64	220	12	0.0246	Forced
	30	0.64	220	8	0.0176	Natural

2.3.2. Product dimension and boundary conditions: case 2 French bread (Purlis and Salvadori, 2009)

The product is French bread (baguette) with uniform irregular cross section (Fig. 2) and length of 8 cm. It is baked for 30 min at different oven temperatures (180, 200 and 220 °C), under forced and natural convection. Convection is adjusted by the modification of convective heat and mass transfer coefficients as detailed in Table 2.

Boundary conditions are the same for surfaces $\partial\Omega_{3,4}$ in Zhang et al. (2005) except for the energy equation, where convective and radiation heat transfer coefficients are considered separately.

$$-k_{eff}\vec{\nabla}T\cdot\vec{n} = h_v(T_{inf}-T_s)+\varepsilon\sigma(T_s^4-T_{inf}^4) \tag{28}$$

2.4. Closure: non equilibrium description of evaporation

The non equilibrium approach, leads to an explicit formulation of $\dot{I}$, Eq. (29) allowing to close the system (Fang and Ward, 1999; Zhang and Datta, 2004)

$$\dot{I} = K\cdot(\rho_{v,eq}-\rho_v) \tag{29}$$

where K is a constant parameter and depends strongly on the operating conditions of the system (ambient fluid, convective heat transfer coefficient, etc.). Since analytical or empirical expressions to calculate K are unavailable, a parameter estimation method was used for its estimation.

$\rho_{v,eq}$ is the density of water vapour at equilibrium and is obtained from the vapour pressure at equilibrium:

$$p_{v,eq} = a_w p_s \tag{30}$$

p_s is the saturation pressure and can be calculated using Clapeyron, Rankine or Duperray equations; a_w is the water activity and was estimated from the expression developed by Lind and Rask (1991), with coefficients revised by Zhang and Datta (2006), i.e.:

$$a_w = \left[\left(\frac{100M}{\exp(-0.0056T+5.5)}\right)^{\frac{-1}{0.38}}+1\right]^{-1} \tag{31}$$

M is the moisture content on dry basis and T is temperature in K.

2.5. Numerical solution

A finite element method was used to solve the system of Eqs. (11), (12), (13), and (18) with initial conditions (19)–(22), and boundary conditions (23)–(28). The numerical procedure was implemented in COMSOL Multiphysics v3.4a software ©. The model was run on a single PC machine, with 2.6 GHz processor and 4 GB RAM. The mesh consists of 1992 and 1198 triangular elements for case 1 and 2, respectively. Tests with finer meshes were made but no influence on the results was observed, which ensured the independence of the results from the mesh. The time step was automatically determined by the software. At each time step, the system of (11), (12), (13), and (18) was solved, seeing the rather simple geometry and low number of mesh cells, a direct solver was used. In Comsol this is typically "Direct UMFPACK". The model thus presented is a system of partial differential equations coupled and strongly nonlinear, which have no analytical solutions. However, a preliminary study on a simple case assuming an analytical solution was considered and is presented in Appendix B. For the simplified situation, the agreement was very good between the analytical and numerical results.

3. Physical and thermal and properties

3.1. Mass transfer properties

3.1.1. Capillary diffusivity of liquid water

Capillary diffusivity due to temperature gradient was neglected, and the following equation for the capillary diffusivity of water (due to concentration gradient only) in bread was used in our model (Zhang et al., 2005):

$$D_w = 10^{-06}\exp(-2.8+2M)\phi \tag{32}$$

3.1.2. Molecular diffusivity of gas

Molecular diffusion in the gas phase depends on the product structure, temperature and water saturation conditions. Since changes of structure during heating are difficult to obtain, it is known that molecular diffusivity decreases with water saturation and increases with temperature in a power law fashion with exponent 1.5 (Datta, 2007b). Zhang et al. (2005) proposed the following expression to calculate this property:

$$D_{eff,g} = D_{vc}[(1-1.11S_w)\phi]^{\frac{3}{4}} \tag{33}$$

where D_{vc} is the binary diffusivity between water vapour and CO_2.

3.1.3. Permeability

Ignoring the volume change of bread during baking, the equivalent porosity was assumed constant. The effect of the structure change (gas porosity, related transport properties) is reflected by variation of permeability (Ni et al., 1999). Permeability of gas is calculated as the product of intrinsic permeability $\kappa_{g,i}$ and relative permeability $\kappa_{g,r}$. The intrinsic permeability of the gas, represents the permeability in a fully saturated state. Zhang et al. (2005) proposed a constant value: $\kappa_{g,i} = 2.5\times10^{-12}$ m^2.

The relative permeability, varies between 0 (none of the phase), and 1 (saturated with the phase), and depends strongly on water content in the product. Ni et al. (1999) proposed a water saturation dependent expression:

$$\kappa_{g,r} = \begin{cases} 1 - 1.1S_w & \text{for } S_w < 0.9 \\ 0 & \text{for } S_w \geqslant 0.9 \end{cases} \quad (34)$$

therefore

$$\kappa_g = \kappa_{g,i}\kappa_{g,r} \quad (35)$$

3.2. Thermophysical properties

The parallel model based on volume fraction (combination of intrinsic properties of each component weighted by its corresponding volume fraction) was used for density ρ_{eff} and specific heat $c_{p_{eff}}$:

$$\rho_{eff} = \rho_s(1-\phi) + \rho_w S_w \phi + \rho_g S_g \phi \quad (36)$$

$$c_{p_{eff}} = c_{ps}(1-\phi) + c_{pw} S_w \phi + c_{pg} S_g \phi \quad (37)$$

For the thermal conductivity, most experimental values (and thus algebraic expressions based on), were obtained for isothermal conditions; however the temperature is an important parameter to assess thermal conductivity. Recently Jury et al. (2007) obtained experimental results of thermal conductivity in pseudo-non-isothermal conditions, these results were fitted by Purlis and Salvadori (2009) and were adopted in our model.

$$k_{eff} = \begin{cases} \frac{0.9}{1+e^{-0.1(T-353.16)}} + 0.2 & \text{if } T \leqslant 99.5\ ^\circ\text{C} \\ 0.2 & \text{if } T > 100.5\ ^\circ\text{C} \end{cases} \quad (38)$$

4. Results and discussion

4.1. Input parameters

The values and the expressions of the model parameters are presented in Table 2.

Table 2
Input parameters used in the model.

Item	Symbol	Value	Source
Thermophysical properties			
Solid density	ρ_s	Eq. (45)	
Vapour density	ρ_v	Ideal gas	
Water density	ρ_w	10^3 (kg m^{-3})	
CO_2 density	ρ_c	Ideal gas	
Specific heat capacity of solid	c_{ps}	1566 (J kg^{-1} K^{-1})	Datta (2007b)
Specific heat capacity of gas	c_{pg}	1006 (J kg^{-1} K^{-1})	Datta (2007b)
Specific heat capacity of water	c_{pw}	4180 (J kg^{-1} K^{-1})	
Thermal conductivity	k_{eff}	Eq. (37)	Purlis and Salvadori (2009)
Latent heat of evaporation	λ	2.435×10^6	Datta (2007a,b)
Mass properties			
Capillary diffusivity coefficient of water	D_w	Eq. (38)	Zhang et al. (2005)
Molecular diffusivity coefficient of vapour and CO_2	$D_{eff,g}$	Eq. (32)	Zhang et al. (2005)
Porosity	ϕ	Eq. (43)	
Gas viscosity	μ_g	1.8×10^{-5} (Pa s)	
Intrinsic permeability of gas	k_{gi}	2.5×10^{-12} (m^2)	Zhang et al. (2005)
Relative permeability of gas	k_{gr}	Eq. (33)	Zhang et al. (2005)
Density of vapour surrounding air	$\rho_{v,\text{inf}}$	0 (kg m^{-3})	Zhang et al. (2005)

4.2. Model validation

In the simplified analytically solved situation of gas diffusion, the model gave satisfactory results; a comparison with the analytical solution has an error of 2% (see Appendix B).

Validation for the short cylindrical bread (case 1) involved the temperature field at the center and surface of the bread and the total moisture content (dry basis). Parametric estimation on evaporation rate constant (Eq. (29)) have shown that $K = 0.1$ gave the lowest difference between estimated and experimental values (Fig. 3a and b). The model reproduces the behavior for the experimental temperature increase and decreasing water content during the process. Quantitatively, the maximum error (Eq. (39)) is about 8.2%, 5.2% and 3% for temperature at the center, surface and the total moisture content, respectively. These errors are mainly at the beginning of the process. Average error (Eq. (40)) is 4.7%, 2.9% and 1.6% for the same variables.

$$er_{\max} = \max\left(100\frac{abs[X^i_{\text{exp}} - X^i_{cal}]}{X^i_{\text{exp}}}\right)_i \quad (39)$$

$$er_{aver} = \frac{1}{n}\sum_{i=1}^{n} 100\frac{abs[X^i_{\text{exp}} - X^i_{cal}]}{X^i_{\text{exp}}} \quad (40)$$

Keeping similar mass and thermal properties relationships and $K = 0.1$, the model was applied to French bread (case 2) for different oven temperatures and convection mode as detailed in Table 1. The

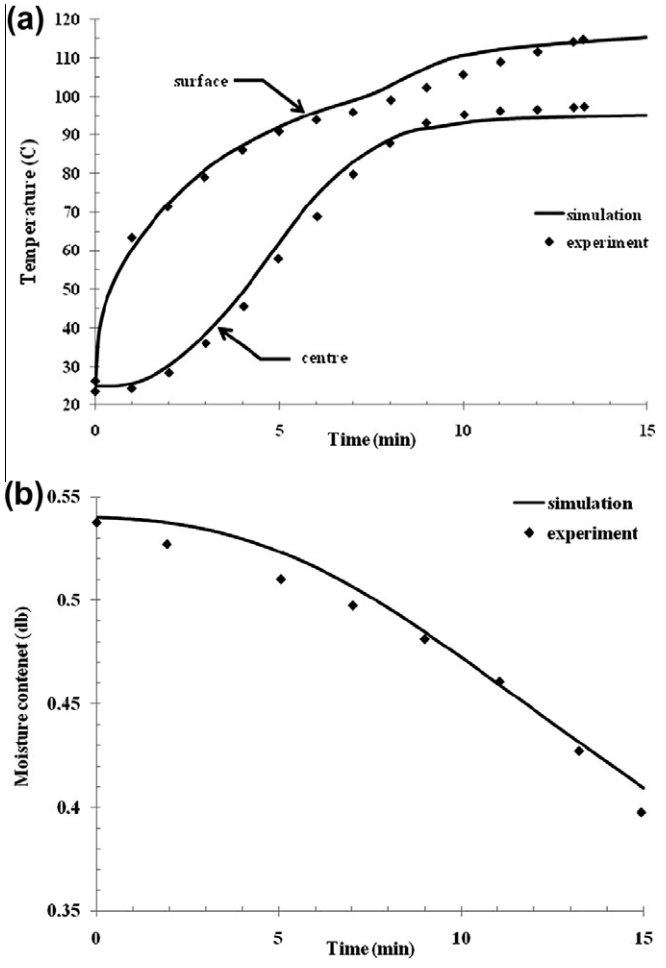

Fig. 3. Results of short cylindrical bread for $K = 0.1$: (a) Temperature evolution at center and surface during baking. (b) Total moisture content evolution during baking.

available data are for the temperature field at the center and the total moisture content (dry basis). A sample of results presented in Fig. 4a and b shows an acceptable correlation between the estimates and experiments. The model underestimates the increase in temperature and decrease of water content, this is due mainly to 3D character of the experiments where the contribution of heat flow in the third dimension (length) was not taken into account by our 2D model. However, the magnitude of the error is acceptable (see Table 3 for more details).

For both types of product considered (cases 1 and 2), the model gives a good description of the two key parameters (moisture and temperature) of the baking process. These results show that the non equilibrium approach describes well the baking process and confirms the work of Zhang et al. (2005), that the vapour pressure is likely to be lower than the equilibrium vapour pressure. In addition, the good agreement between the estimated and the experimental transient temperature and moisture content profiles confirm that neglecting the volume change during the process was an appropriate assumption. However, the volume change is important to include for the analysis of product quality (limit swelling to avoid damaging texture or limit crust formation).

The convection mode has no significant influence on the evaporation rate constant, this is firstly due to the minor role played by convection in baking process as compared to radiation (Baik et al., 1999). Secondly, the difference between convective heat transfer coefficient in forced and natural convection mode does not exceed 50% (see Purlis and Salvadori, 2009). For processes where the convective heat transfer coefficient is large (≈400 W/m^2 K in the case of frying) previous work showed that K is about 100 s (Halder et al., 2007b).

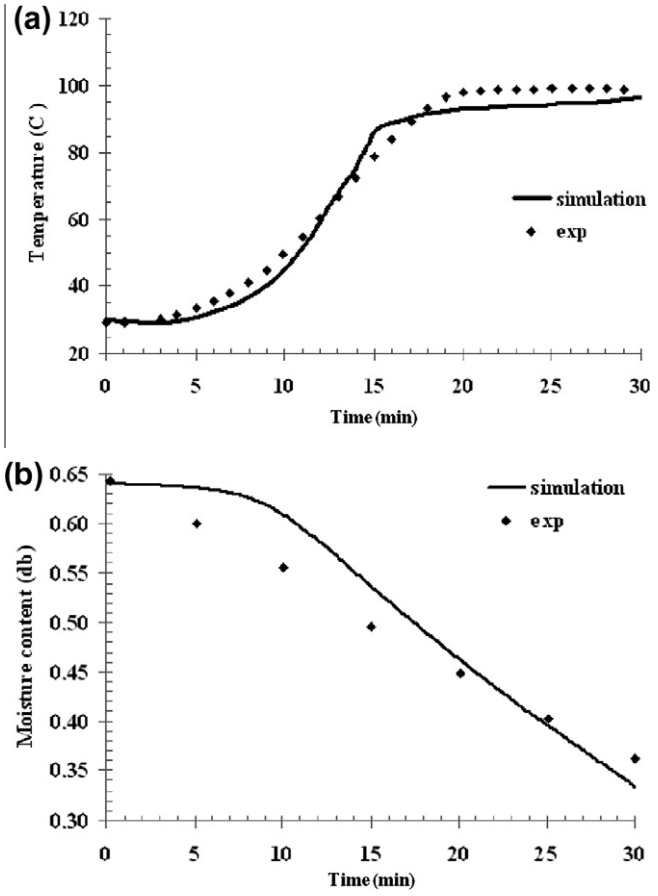

Fig. 4. Results of French bread for $K = 0.1$: (a) Temperature evolution at center for natural convection $T_{oven} = 220$ °C. (b) Total moisture content evolution for forced convection $T_{oven} = 180$ °C.

Table 3
Maximum and average errors between experiments and simulations for $K = 0.1$ for case 2.

T_{inf}°C convection mode	$er_{max\%}$		$er_{aver\%}$	
	Temperature at the center	Total moisture content	Temperature at the center	Total moisture content
180, forced	N/A	9.4	N/A	5.7
200, forced	16.4	7.1	10	5.2
220, forced	N/A	13	N/A	5
220, natural	11.5	N/A	5.2	N/A

4.3. Distribution of convective and diffusive flux of water vapour

In this section and the following, our study is limited to the short cylindrical bread (case 1) for simplicity, knowing that the observations and conclusions remain valid for the French bread (case 2).

The convective flux (Fig. 5a) is mainly occurring near the surface (≈1 cm from surface), where there is an important pressure gradient. At the beginning of the baking process, there is no convective flux away from the surface since the pressure is nearly constant. During the baking process, the convective flux is much lower in the center than near the surface because of the small pressure gradient in the center of the product. The maximum of the convective flux shifts towards the center and reached its highest value at $t = 10$ min when the evaporation rate is maximum. The negative values estimated at $t = 5$ min, correspond to the condensation as observed by De Vries et al. (1989) and Thorvaldsson and Skjöldebrand (1998)) and illustrated by Fig. 5b, presenting the direction of water vapour convective flux at the same time (5 min). Indeed, at this stage of the process, the water vapour that moves toward the center will be located in areas where the temperature is well below the melting temperature and thus condensation occurs.

As shown in Fig. 5c, the water vapour diffuses towards the surface. The maximum of the diffusive flux is located at the surface for different times, due to the significant gradient between the vapour density at the surface (increasing with temperature) and the surrounding air where ρ_v is very low and estimated as zero in our simulation. The diffusive flux decreases in the direction of the center, because of the decreasing molecular diffusivity of vapour water. As for the convective flux, the condensation is observed in the center of bread at the beginning of the process, which is consistent with the results of Thorvaldsson and Janestad (1999).

4.4. Sensitivity analysis

In the present and subsequent sections, we investigate the influence of operating conditions on the final state of the product. The parametric study was implemented using the same geometry used in the experimental work of Zhang et al. (2005). The parametric study conclusions remain valid for the work of Purlis and Salvadori (2009).

Operating conditions (oven temperature) and product formulation (initial moisture content), strongly influences the product quality. Indeed the texture (crumb, crispiness, softness) depends among other properties on the moisture content of the product (Hadiyanto et al., 2008) and the color (Maillard reactions) which is developed according to the surface temperature of the product (Zanoni et al., 1994). The advantage of modeling is the ability to predict the impact of different oven operating conditions on the

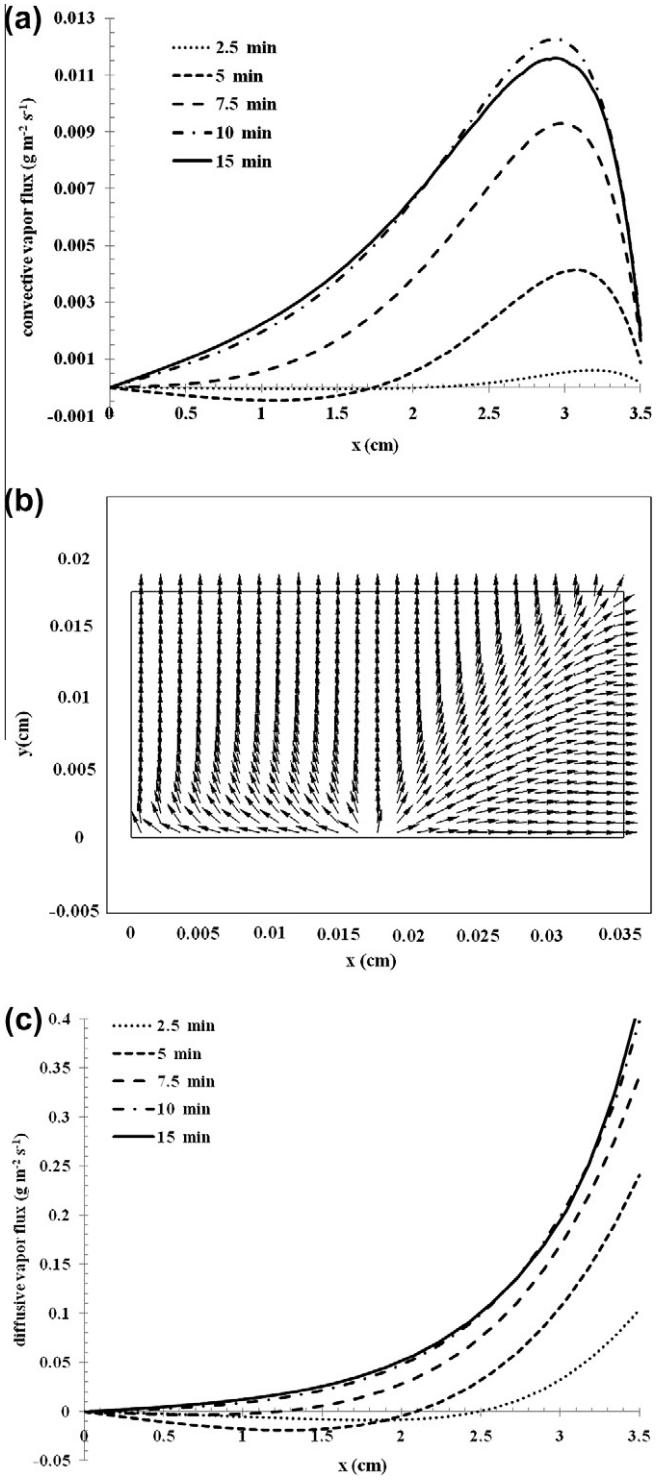

Fig. 5. Analysis of convective and diffusive water vapour flux ($K = 0.1$): (a) Convective water vapour flux at different positions in the baking product and for different baking times. (b) Water vapour flow direction in the bread baking product ($t = 5$ min). (c) Diffusive water vapour flux at different positions in the bread baking product and for different baking times.

quality parameters for different baking product formulations without having to carry costly and complicated experimentation.

In this section, the effect of the value for constant K, the oven temperature, the product initial moisture content and the convective heat transfer coefficient on the temperature in the product will be analyzed. As the empirical measurement of the constant K in (Eq. (29)) is difficult, the sensibility of the prediction (moisture and temperature) to the value of K will be also investigated.

4.4.1. Impact of non equilibrium evaporation constant "K" on temperature and moisture content fields

The non equilibrium evaporation constant "K" is a critical parameter in the model developed in this study. Since no studies to quantify this parameter for baking process was available, we have considered the only study available, a frying process carried out by Halder et al. (2007b). These authors tested a range of K values, from 1 to 1000, and concluded that the value 100 s^{-1} was the most appropriate to obtain the best fit between the model estimates and the experimental values of moisture and temperature during the process (Halder et al., 2007a). In our case, the preliminary studies showed that K values near 1 s^{-1} were more adequate. Fig. 6a shows the temporal evolution of temperature at the center of the product for different values of K (0.1; 0.2; 0.5; 1). In the four cases, the model reproduced typical evolution of temperature with phase change, characterized by a quick rise at the beginning, followed by a pseudo plateau where no pronounced variation of temperature occurred.

For lower values of K (0.1; 0.2) the temperature increase was more important, due particularly to the low value of the source term $\lambda \dot{I}$ in the energy equation (Eq. (18)). For higher K values (0.5; 1); this term is more important and therefore, more energy is devoted to evaporation.

Eq. (29) used for calculation of $\dot{I}$ shows that this parameter depends on the temperature and moisture content of the product. This dependence is illustrated in Fig. 6b, and shows the evolution of the average evaporation rate (Eq. (41)) for different values of K. For all K values investigated, $\langle \dot{I} \rangle$ increases with time due essentially to the temperature increase allowing more liquid water to evaporate. This increase reaches a maximum and then the decrease is a consequence of the low liquid water concentration remaining.

$$\langle \dot{I} \rangle = \frac{\int_{\Omega} \dot{I} \cdot dV}{V} \tag{41}$$

The increase was more pronounced for high K values (1; 0.5) where average of evaporation rate reached a maximum (≈ 0.5 kg m^{-3} s^{-1}) at $t = 8$ min and 10 min, respectively. For the lower K values (0.1; 0.2), the increase was less important (max ≈ 0.38, and 0.42 kg m^{-3} s^{-1}), respectively, and took more time to be reached: 11 min for $K = 0.2$ and 12 min for $K = 0.1$.

Similarly for the total moisture content (Fig. 6c), the decrease was more pronounced for high K values, because $\dot{I}$ is more important.

4.4.2. Effect of oven temperature

A range of oven temperatures (180–200 °C) was chosen, because these temperatures are typical in the bread baking industry (Le-Bail et al., 2009). Fig. 7a shows the temporal evolution of the temperature at the center and the surface of the product. As expected, the product temperature increases with increasing oven temperature; however, the increase is not proportional to the increment. The oven temperature effect starts at the surface (soon as $t = 2$ min), since the region where the baking product is directly in contact with the oven environment. At the center of the product, the thermal resistance of the product and the latent heat of water evaporation slows the heat flux, and the effect of the oven temperature became visible only after $t = 5$ min. The effect on the moisture content (Fig. 7b) is similar to the effect on the center temperature, with negligible effect during the first five minutes, after the moisture content decreases with increasing oven temperature.

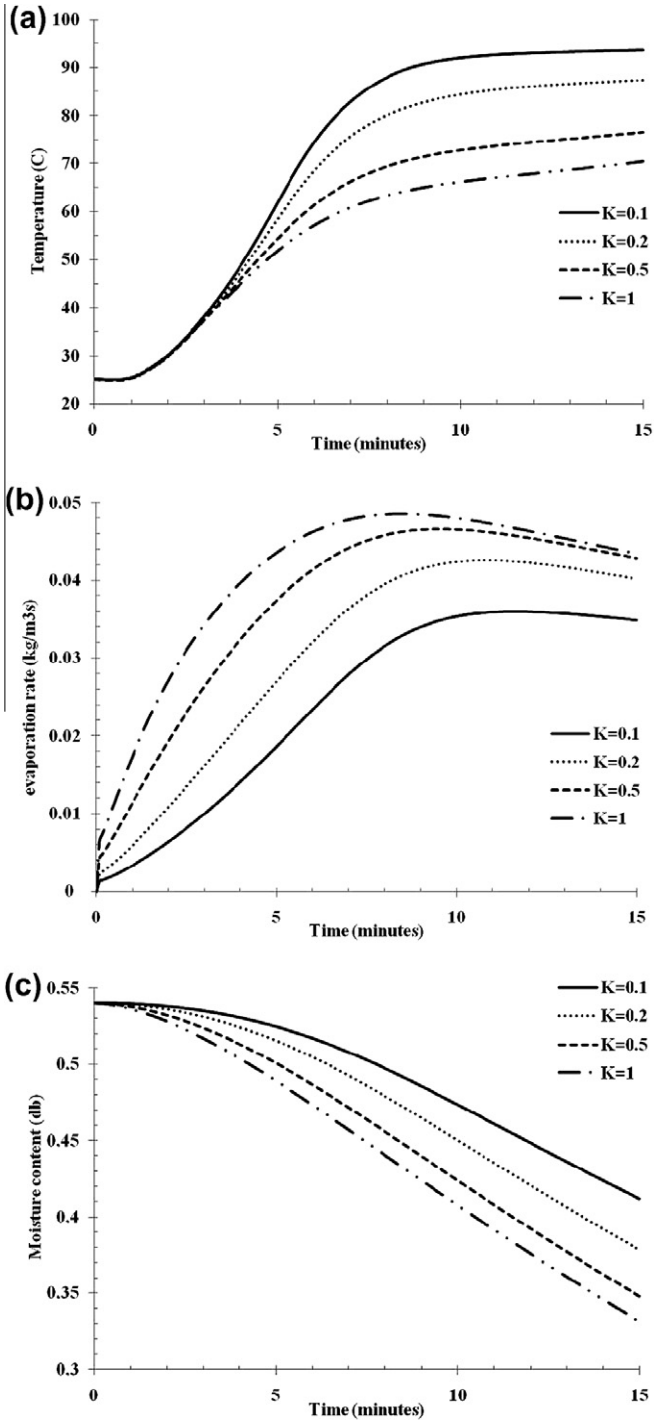

Fig. 6. Impact of evaporation rate constant K on: (a) Temperature in the center of the bread baking product. (b) Average evaporation rate of the bread baking product. (c) Total moisture content of the bread baking product.

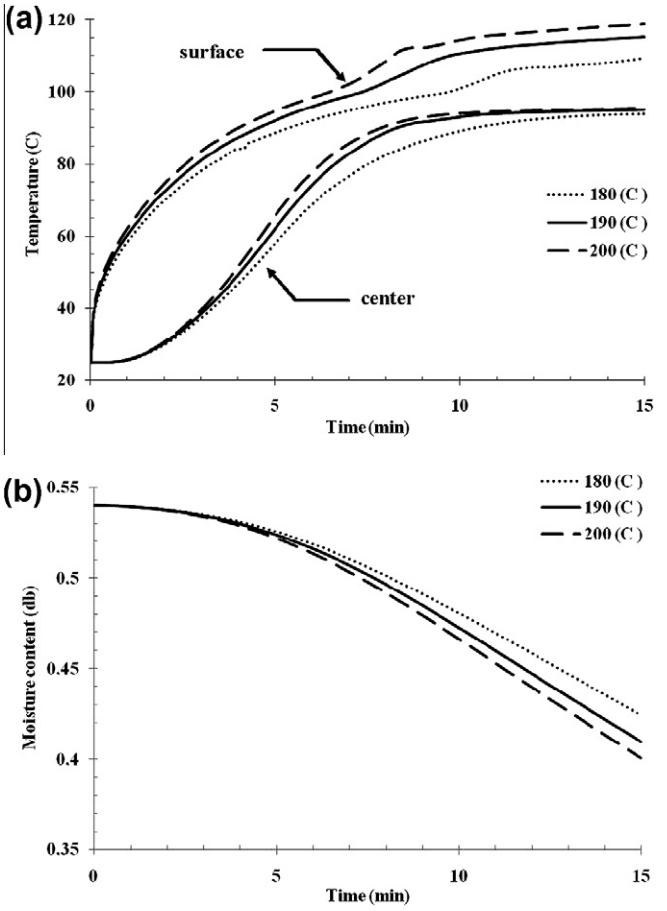

Fig. 7. Effect of oven temperature ($K = 0.1$) on: (a) Temperature field at center and surface of the bread baking product. (b) Total moisture of the bread baking product.

4.4.3. Effect of the oven convective heat transfer coefficient (h_t)

According to the results presented in Fig. 8a and b, the heat transfer coefficient is the most important parameter on the product temperature and moisture content. Fig. 8a shows that the temperature increases with increasing h. The difference is relatively small for h, between 15 and 20 W m^{-2} K^{-1}, due to the thermal resistance of the product (limitation of conduction heat flux). Similarly, the product moisture content decreases quickly with increasing h (Fig. 8b). This information is important from an energy point of view, that if we need to increase heating, it is more efficient to improve the convective heat transfer coefficient (by increasing the hot air flow, for example), than increasing the oven temperature. From a product quality point of view, the surface temperature for h = 20 W m^{-2} K^{-1} reaches temperature of 140 °C at the end of the process. But this temperature corresponds to conditions where the surface of the bread will have burned, so the optimal value regarding this constraint will be h value near 15 W m^{-2} K^{-1}, we will save time (energy) of process duration, and the quality will be acceptable also.

5. Conclusion

A 2D model describing the heat and mass transfer for bread baking was proposed. It takes into account the structure of the product, the diffusive and the convective mechanisms for the gas phase and the evaporation condensation associated with conduction for heat transfer. For the liquid phase, neglecting convection mass transfer and taking into account only capillary diffusion due to concentration gradient was found to be an appropriate assumption.

The use of the non equilibrium approach, allows the implementation of the model in commercial software, therefore to explore more practical situations of product, process and equipment design.

Three study cases were investigated for the model verification and quantification of the constant rate of evaporation (K). The first study concerns a simple case of gas diffusion that admits an analyt-

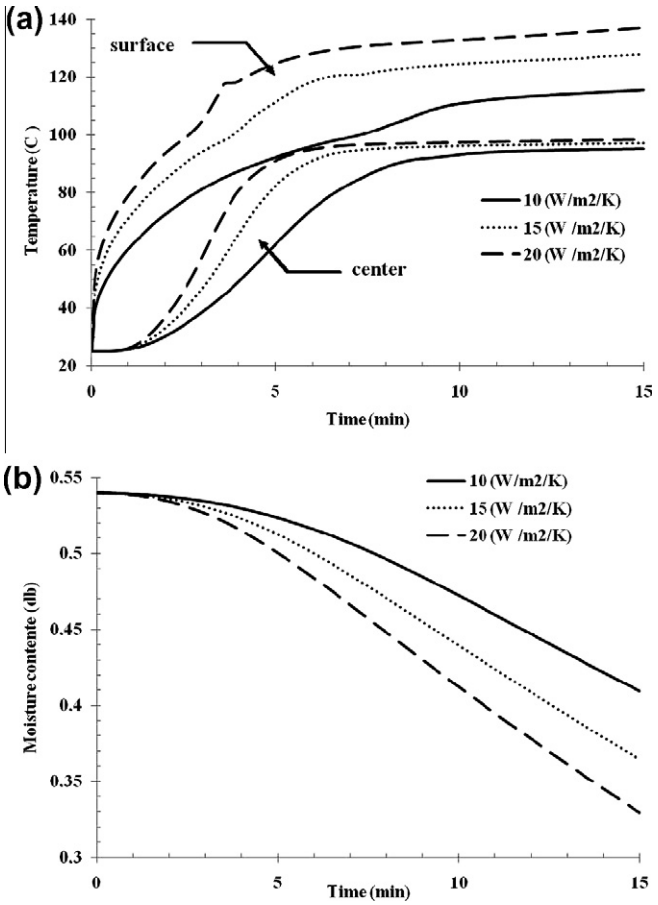

Fig. 8. Effect of convective heat transfer coefficient ($K = 0.1$) on: (a) Temperature field at center and surface of the bread baking product. (b) Total moisture total moisture content of the bread baking product.

ical solution. The second and third tests were conducted on the experimental data of real product (bread) baking to pilot scale. Different operating conditions have been investigated (natural convection, forced convection).

Comparison were mainly in the fields of temperature and moisture content and showed that low values of K (evaporation rate constant) are the most appropriate to represent the experimental temperature and moisture measurements of the baking product. This confirms the previous studies showing that vapour pressure is likely to be lower than the equilibrium water vapour pressure.

The analysis of the magnitude of the different mass transfer mechanisms showed that convective mass transfer of the vapour inside the bread is less than the diffusive mass transfer. Therefore one can neglect this term which will facilitate the resolution of complex applications "inverse method to determine the constant rate of evaporation" for example.

Finally, a sensitivity analysis of the initial and operating conditions shows that baking process is affected mainly by the convective heat transfer and the product initial moisture characteristics.

Future work will be oriented towards the development of a more precise estimation of the evaporation rate constant (using inverse method) and the implementation of the parameters associated with the product quality and their optimization.

Acknowledgements

This project is part of the R&D program of the NSERC Chair in Industrial Energy Efficiency established in 2006 at "Université de Sherbrooke". The authors acknowledge the support of the Natural Sciences & Engineering Research Council of Canada, Hydro Québec, Rio Tinto Alcan and CANMET Energy Technology Center.

Appendix A

A.1. Calculation of the initial values

In most cases the data available are the moisture content on dry basis (db) (Eq. (42)) the initial density of dough ρ_o, and the initial gas volume ratio $\frac{V_g}{V_{tot}} = 0.61$ as reported by Zanoni et al. (1995):

$$M_0 = \frac{m_{H_2O}}{m_{db}} \tag{42}$$

Rq: In some cases we have the initial moisture content on wet basis (wt), i.e.: $M_0 = \frac{m_{H_2O}}{m_{product}}$, we can easily deduce the value of M_0 by Eq. (43)

$$M_0 = \frac{M_{wt}}{1 + M_{wt}} \tag{43}$$

A.2. Calculation of the apparent porosity

$$\rho_0 = \frac{m_{H_2O} + m_{db}}{V_{tot}}, \quad \text{with } m_{db} = \frac{m_{H_2O}}{M_0} \Rightarrow \rho_0 = \frac{m_{H_2O}}{V_{tot}}\left(1 + \frac{1}{M_0}\right) = \frac{m_{H_2O}}{V_{tot}}\left(\frac{M_0 + 1}{M_0}\right)$$

$$\rho_0 = \frac{V_w}{V_{tot}}\rho_w\left(\frac{M_0 + 1}{M_0}\right) = \left(\phi - \frac{V_g}{V_{tot}}\right)\rho_w\left(\frac{M_0 + 1}{M_0}\right) \Rightarrow \phi - \frac{V_g}{V_{tot}} = \frac{\rho_0}{\rho_w}\left(\frac{M_0}{M_0 + 1}\right)$$

And finally

$$\phi = \frac{V_g}{V_{tot}} + \frac{\rho_0}{\rho_w}\left(\frac{M_0}{M_0 + 1}\right) \tag{44}$$

A.3. Calculation of the initial water saturation

The initial gas volume ratio is defined as $\frac{V_g}{V_{tot}} = \phi S_g = \phi(1 - S_w)$ so:

$$S_{w0} = 1 - \frac{1}{\phi}\frac{V_g}{V_{tot}} \tag{45}$$

A.4. Calculation of the density of dry flour

$$\rho_s = \frac{\rho_w S_w \phi}{M_0(1 - \phi)} \tag{46}$$

Appendix B

B.1. Analytical solution of the simplified formulation

The simplified formulation corresponds to a linear model where the equations are not coupled. Furthermore, all properties are considered constant and based on the values of Hadiyanto et al. (2007). The simplified formulation is for the diffusion equation of water vapour (Eq. (2)) and uniform and constant temperature field was considered. The geometry, initial and boundary conditions are identical to case 1.

Let us take $\rho_v \phi S_g = \rho_s V$, and consider that the transfer is made only by diffusion, Eq. (12) and can be rewritten as:

$$\left[\rho_s \frac{\partial V}{\partial t} = \rho_s \vec{\nabla} \cdot (D_{eff} \vec{\nabla} V) + K\rho_s(V_{eq} - V)\right]$$

The initial condition is:

$$V(0, r, z) = V_0$$

All the physical properties are assumed constant during the baking process and the vapors V_{eq} and V_{ext} are equal and constant.

The boundary conditions:

$$-\rho_s D_{eff}\nabla V(t,r,0) = 0$$
$$-\rho_s D_{eff}\nabla V(t,r,H) = \rho_s h_v (V(t,r,H) - V_{ext})$$
$$-\rho_s D_{eff}\nabla V(t,R,z) = \rho_s h_v (V(t,R,z) - V_{ext})$$
$$-\rho_s D_{eff}\nabla V(t,0,z) = 0$$

As the partial differential equation is linear and homogeneous with the change of variable $V' = V - V_{ext}$, the method of variable separation was used with the mix of Newman and mixed boundary conditions. The solution is a sum of Bessel and cosinus functions:

$$V(t,z,r) = V_{ext} + \sum_{n=1}^{\infty}\sum_{m=1}^{\infty} a_{n,m} J_0(\lambda_n r)\cos(\gamma_m z) e^{-\alpha^2 D_{eff} t}$$

$$\alpha^2 = \lambda_n^2 + \gamma_m^2 + K$$

$$\text{with} \quad (\lambda_n R) J_1(\lambda_n R) = Cr J_0(\lambda_n R), \quad Cr = \frac{R h_v}{D_{eff}}$$

$$\text{with} \quad (\gamma_m H)\sin(\gamma_m H) = Cz\cos(\gamma_m H), \quad Cz = \frac{H h_v}{D_{eff}}$$

$$a_{n,m} = \frac{2Cr}{R^2(\lambda_n^2 + Cr^2) J_0(\lambda_n R)} \frac{2\sin(\gamma_m H)}{\cos(\gamma_m H)\sin(\gamma_m H) + \gamma_m H}$$

The series converges and the first few terms are significant. The two equations (for Bessel and trigonometric function) have an infinite number of roots and the roots are increasing. The first roots are given by Carslaw and Jaeger (1959) for different values of *Cr* and *Cz*. With five roots for the analytical solution, the comparison with the numerical solution provided by Comsol gives the same result with 2% error.

References

Baik, O.D., Sablani, S.S., Marcotte, M., Castaigne, F., 1999. Modeling the thermal properties of cup cake during baking. Journal of Food Science 64 (2), 295–299.

Bear, J., 1972. Dynamics of Fluids in Porous Media. American Elsevier Publishing Company, Inc., New York, NY.

Bird, R.B., Stewart, W.E., Lightfoot, E.N., 2001. Transport Phenomena, second ed. Wiley, New York.

Carslaw, H.S., Jaeger, J.C., 1959. Conduction of Heat in Solids. Oxford University Press.

Datta, A.K., 2007a. Porous media approaches to studying simultaneous heat and mass transfer in food processes. I: problem formulations. Journal of Food Engineering 80 (1), 80–95.

Datta, A.K., 2007b. Porous media approaches to studying simultaneous heat and mass transfer in food processes. II: property data and representative results. Journal of Food Engineering 80 (1), 96–110.

De Vries, U., Sluimer, P., Bloksma, A.H., 1989. A quantitative model for heat transport in dough and crumb during baking. Cereal Science and Technology, Sweden, Asp, NG, pp. 174–188.

Fang, G., Ward, C.A., 1999. Examination of the statistical rate theory expression for liquid evaporation rates. Statistical physics, plasmas, fluids, and related interdisciplinary topics. Physical Review E 59 (1), 441–453.

Fellows, P.J., 1996. Food Processing Technology Principles and Practice. Woodhead Publishing, Cambridge.

Hadiyanto, A. Asselman, van Straten, G., Boom, R.M., Esveld, D.C., van Boxtel, A.J.B., 2007. Quality prediction of bakery products in the initial phase of process design. Innovative Food Science & Emerging Technologies 8 (2), 285–298.

Hadiyanto, D.C. Esveld, Boom, R.M., van Straten, G., van Boxtel, A.J.B., 2008. Product quality driven design of bakery operations using dynamic optimization. Journal of Food Engineering 86 (3), 399–413.

Halder, A., Dhall, A., Datta, A.K., 2007a. An improved, easily implementable, porous media based model for deep-fat frying. Part I: model development and input parameters. Food and Bioproducts Processing 85 (3), 209–219.

Halder, A., Dhall, A., Datta, A.K., 2007b. An improved, easily implementable, porous media based model for deep-fat frying. Part II: results, validation and sensitivity analysis. Food and Bioproducts Processing 85 (3), 220–230.

Huang, H., Lin, P., Zhou, W., 2007. Moisture transport and diffusive instability during bread baking. SIAM Journal of Applied Mathematics 68, 222–238.

Jury, V., Monteau, J.-Y., Comiti, J., Le-Bail, A., 2007. Determination and prediction of thermal conductivity of frozen part baked bread during thawing and baking. Food Research International 40 (7), 874–882.

Le-Bail, A., Boumali, K., Jury, A., Ben-Aissa, A., Zuniga, R., 2009. Impact of the baking kinetics on staling rate and mechanical properties of bread crumb and degassed bread crumb. Journal of Cereal Science 50 (2), 235–240.

Lind, I., Rask, C., 1991. Sorption isotherms of mixed minced meat, dough, and bread crust. Journal of Food Engineering 14 (4), 303–315.

Mondal, A., Datta, A.K., 2008. Bread baking – a review. Journal of Food Engineering 86 (4), 465–474.

Ni, H., Datta, A.K., Torrance, K.E., 1999. Moisture transport in intensive microwave heating of wet materials: a multiphase porous media model. International Journal of Heat and Mass Transfer 42, 1501–1512.

Purlis, E., Salvadori, V.O., 2009. Bread baking as a moving boundary problem. Part 2: model validation and numerical simulation. Journal of Food Engineering 91 (3), 434–442.

Thorvaldsson, K., Janestad, H., 1999. A model for simultaneous heat, water and vapour diffusion. Journal of Food Engineering 40 (3), 167–172.

Thorvaldsson, K., Skjöldebrand, C., 1998. Water diffusion in bread during baking. Lebensmittel-Wissenschaft und-Technologie 31 (7–8), 658–663.

Zanoni, B., Peri, C., Pierucci, S., 1994. Study of the bread baking process II. Mathematical modelling. Journal of Food Engineering 23 (3), 321–336.

Zanoni, B., Peri, C., Gianotti, R., 1995. Determination of the thermal diffusivity of bread as a function of porosity. Journal of Food Engineering 26 (4), 497–510.

Zhang, J., Datta, A.K., 2004. Some considerations in modeling of moisture transport in heating of hygroscopic materials. Drying Technology 22 (8), 1983–2008.

Zhang, J., Datta, A.K., 2006. Mathematical modeling of bread baking process. Journal of Food Engineering 75 (1), 78–89.

Zhang, J., Datta, A.K., Mukherjee, S., 2005. Transport processes and large deformation during baking of bread. AIChE Journal 51 (9), 2569–2580.

Zhang, L., Lucas, T., Doursat, C., Flick, D., Wagner, M., 2007. Effects of crust constraints on bread expansion and CO_2 release. Journal of Food Engineering 80 (4), 1302–1311.

Zhou, W., 2005. Application of FDM and FEM in solving the simultaneous heat and moisture transfer inside bread during baking. International Journal of Computational Fluid Dynamics 19 (1), 73–77.